Heat Treatment Effects on Creep and Rupture Behavior of Annealed 2.25 Cr-1 Mo Steel

R. L. KLUEH

The strength of 2 1/4 Cr-1 Mo steel depends on the microstructure, which, in turn, depends on the heat treatment. In the fully annealed and isothermally annealed conditions, the microstructure is primarily proeutectoid ferrite with varying amounts of bainite and pearlite. The relative amounts of the latter constituents depend on the cooling rates during the anneal. The creep and rupture properties were determined for steel plates (from a single heat) given three different annealing treatments: two were fully annealed, but cooled at different rates from the austenitizing temperature, and the third was isothermally annealed. Properties were determined at 454, 510, and 566°C. At 454 and 510°C, the cooling rate had a significant effect on the creep and rupture properties, with the material cooled fastest being the strongest. Although at 510°C strengths at short rupture times differed widely, the properties approached a common value at longer rupture times. The properties differed very little at 566°C, even for short rupture times. The effect of heat treatment was concluded to be the result of interaction solid solution hardening, a dislocation-drag process. This process gave rise to nonclassical creep curves (as opposed to classical curves with single primary, secondary, and tertiary stages). By examining the creep-curve shape, it was possible to interpret the heat treatment effects on the creep-rupture properties.

ANNEALED 2 1/4 Cr-1 Mo steel is being considered as structural material for the steam generators of Breeder Reactors. It is also in common use in fossil fueled power generation systems. Two types of annealing treatments are commonly used for this steel:[1,2] a full anneal and an isothermal anneal. Both heat treatments give a microstructure that is primarily proeutectoid ferrite. Previously we investigated the effect of heat treatment on tensile properties, and a definite effect was observed.[1] The objective of this study was an investigation of the effect of the annealing treatment on the creep and creep-rupture properties.

EXPERIMENTAL

Three sections of a 25 mm thick steel plate taken from a single heat (B and W 20017) were tested (Table I). Two sections were given different full anneals (different furnace cooling rates) and one was given an isothermal anneal. The fully annealed sections were austenitized 1 h at 927°C and then furnace cooled at different rates. The other section was isothermally annealed by furnace cooling from 927 to 704°C at about 83°C/h, holding at that temperature for 2 h, then furnace cooling (Fig. 1). For comparison, the curve for the air-cooled plate (normalized) is also shown in Fig. 1. Hereafter, the two annealed plates will be referred to as AN-1 and AN-2 (AN-2 was cooled faster than AN-1), and the isothermally annealed plate as IA. Most of our tests were made on AN-1 and IA.

The microstructures of the steel in these three heat-treated conditions were previously discussed.[1] After all three heat treatments, the microstructures were primarily proeutectoid ferrite with some pearlite and bainite. Heat treatments AN-1, AN-2, and IA were estimated to have respectively 20, 25, and 20 pct bainite and 1, < 1, and 1 pct pearlite.

Table I. Chemical Composition of 25 mm Plate of Annealed 2 1/4 Cr-1 Mo Steel

	Chemical Composition, Wt Pct							
Analysis	C	Mn	Si	Cr	Mo	Ni	S	P
Vendor	0.11	0.55	0.29	2.13	0.90		0.014	0.011
ORNL	0.135	0.57	0.37	2.2	0.92	0.16	0.016	0.012

For the constant-load creep-rupture tests at 454, 510, and 566°C, specimens with a 6.4 mm diam × 63.5 mm long reduced section were used. The tests were made in air on constant load lever-arm creep frames with 12/1 and 20/1 ratios; the specimens were heated by a Marshall resistance furnace. During test the temperature was monitored and controlled by three

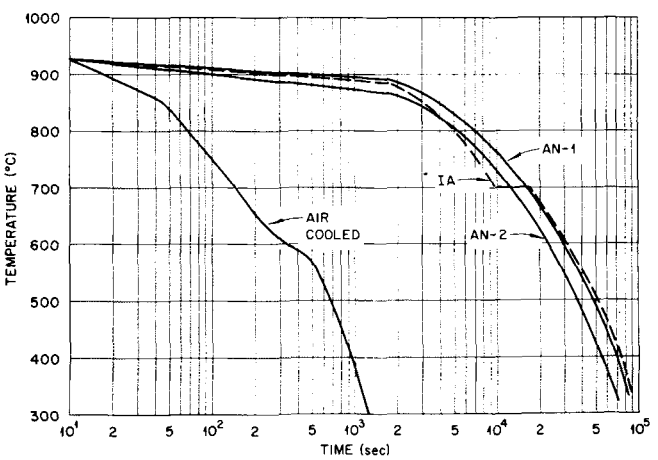

Fig. 1—Cooling curves for the three different annealed heat treatments used on the plates. For comparison, the curve for an air-cooled normalized plate is also shown.

R. L. KLUEH is Research Metallurgist, Metals and Ceramics Division, Oak Ridge National Laboratory, Oak Ridge, TN 37830.

Manuscript submitted April 10, 1978.

ISSN 0360-2133/78/1113-1591$00.75/0

Chromel-Alumel thermocouples attached along the specimen gage section. Temperatures were controlled to ±1°C, and the temperature varied less than ±2°C along the gage section. Creep strains were measured with a mechanical extensometer attached to the specimen shoulders, and the strain was read periodically on a dial gage with a sensitivity of 0.3 μm.

RESULTS

Rupture Life and Minimum Creep Rate

The results for the creep-rupture tests for AN-1, AN-2, and IA are given in Tables II to IV, respectively, while Fig. 2 shows the creep-rupture curves for the three heat treatments. Creep-rupture tests were made over a range of stresses at all three temperatures for AN-1 and IA, with the most detailed work being done on AN-1 (considerable low-stress creep data are being obtained on AN-1 and will be reported at a later date). For AN-2, a creep-rupture curve was obtained only at 510°C, with some comparative tests made at the other two temperatures.

Several points are of interest from Fig. 2. At 510°C at the high stresses, the properties of AN-2—the fast-cooled anneal—and the other two heat treatments obviously differ. At lower stresses, however, the properties for AN-2 approach those of the other two heat treatments. At both 510 and 566°C, the properties for AN-1 are slightly above those for IA, but as the stress is decreased, the rupture times for these two steels also approach one another. At 566°C the approach of properties is complete by about 10^3 h (at 124 MPa the rupture life for AN-2 was less than that for AN-1, and at 103 MPa, the rupture life for IA exceeded that for AN-1). At 454°C, where only AN-1

Table II. Creep-Rupture Properties of Annealed (AN-1) 2¼ Cr-1 Mo Steel

Stress, MPa	Rupture Life, h	Elongation, Pct	Reduction, of Area, Pct	Minimum Creep Rate, Pct/h
		454°C		
327	12059.1	16.0	68.7	0.0000957
358	1435.3	17.2	70.8	0.00142
379	539.1	18.5	71.4	0.0056
413	233.4	19.2	64.4	0.0148
448	48.9	17.3	66.4	0.062
		510°C		
152	9650.3	32.8	69.6	0.000125
172	*			0.0005
172	2788.0	36.4	76.1	0.00053
189	1396.4	35.6	81.4	0.00125
207	1089.3	34.7	82.3	0.0025
241	476.0	26.4	77.0	0.0043
276	135.5	28.8	76.3	0.0243
310	47.5	24.4	76.0	0.069
		566°C		
103	8194.8	18.6	47.0	0.00065
124	1804.6	27.9	66.1	0.0055
138	707.3	31.2	77.9	0.00187
138	885.4	32.3	71.7	0.0033
152	222.9	46.4	82.3	0.086
172	78.2	35.2	83.9	0.0375
172	136.5	34.0		0.0196
207	16.3	40.2	85.1	0.51

*Test discontinued after 1321.3 h and 3.1 pct elongation.

Table III. Creep-Rupture Properties of Annealed (AN-2) 2¼ Cr-1 Mo Steel

Stress, MPa	Rupture Life, h	Elongation, Pct	Reduction of Area, Pct	Minimum Creep Rate, Pct/h
		510°C		
152	*			0.0000267
207	2372.8	32.3	75.8	0.000168
207	2354.4	28.4	78.1	0.000167
276	952.9	22.8	73.4	0.00101
310	563.0	20.4	70.0	0.0029
345	308.4	19.9	61.1	0.00848
378	220.0	27.4	67.8	0.0165
		566°C		
124	1798.5	35.0	70.9	0.00427
138	982.2	33.4	73.0	0.00267

*Test discontinued before rupture.

Table IV. Creep-Rupture Properties of Isothermally Annealed 2¼ Cr-1 Mo Steel

Stress, MPa	Rupture Life, h	Elongation, Pct	Reduction of Area, Pct	Minimum Creep Rate, Pct/h
		454°C		
276	4131.5	24.6	72.5	0.00024
296	2487.2	23.0	73.1	0.000426
338	1301.9	23.2	70.3	0.00104
358	854.9	17.5	70.4	0.00253
379	479.1	24.3*	67.7	0.00538
413	214.6	15.7	63.2	0.00908
		510°C		
152	6853.9	32.4	78.7	0.000165
172	1879.5	43.2	84.6	0.000462
207	526.0	39.3	81.7	0.00339
241	204.5	43.7	79.6	0.00967
276	74.2	22.4	72.9	0.0397
		566°C		
103	9918.7	23.0	51.0	0.000605
124	1233.1	25.8	76.9	0.00723
138	400.4	47.5	80.0	0.0322
172	68.5	48.2	85.9	0.136

*Failure occurred near end of gage section; the specimen also had a neck (reduced section) near center of gage section with a reduction of area of about 20 pct. Thus, the true "total elongation" is less than 24.3 pct.

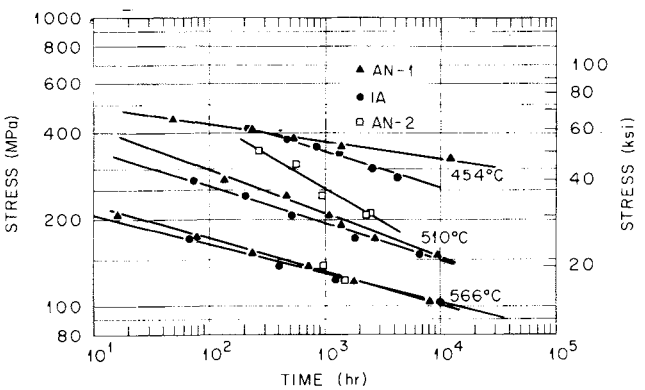

Fig. 2—Creep-rupture curves for 2 1/4 Cr-1 Mo steel at 454, 510, and 566°C; three different heat treatments were tested.

and IA data were obtained, the curves for the two appear to deviate as the stress is decreased.

In Fig. 3 the stress is plotted against the minimum creep rate, and in general, the results parallel the rupture life results. At 454°C (Fig. 3(*a*)), the AN-1 and IA creep rates again deviate with decreasing stress, while at 510°C (Fig. 3(*b*)), the creep rates for these two heat treatments approach one another, especially at the low stresses. For AN-2 the creep rates are considerably less than those for IA and AN-1, but there are again indications that the curves for AN-2 will approach those for the other two heat treatments at low stresses.

At 566°C (Fig. 3(*c*)) the AN-1 and IA results show an apparent discontinuity. That is, an extension of the curve through the creep rates determined for stresses of 103 and 124 MPa would predict a creep rate of about 0.015 at 138 MPa, and little difference between AN-1 and IA. The observed value for AN-1 is about an order of magnitude lower than this, while that for IA is half a log cycle lower. Furthermore, the observed creep rates for the 138 MPa tests are less than those for the 124 MPa tests, certainly an unexpected result.

To try to understand the results, we closely examined the creep curves for each of the above tests, and it was immediately obvious that not all the curves had the classical shape (Fig. 4(*a*)) with primary

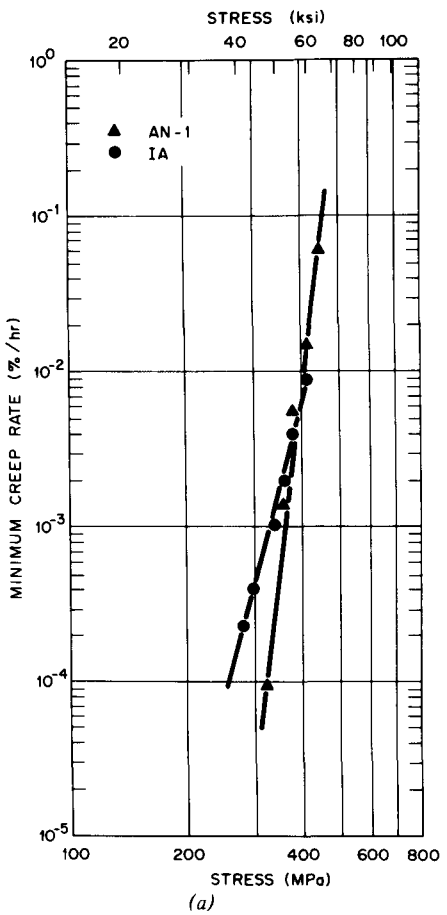

(*a*)

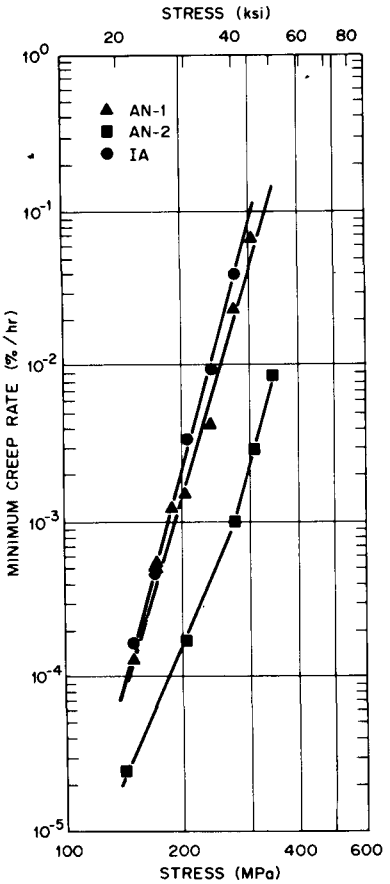

(*b*)

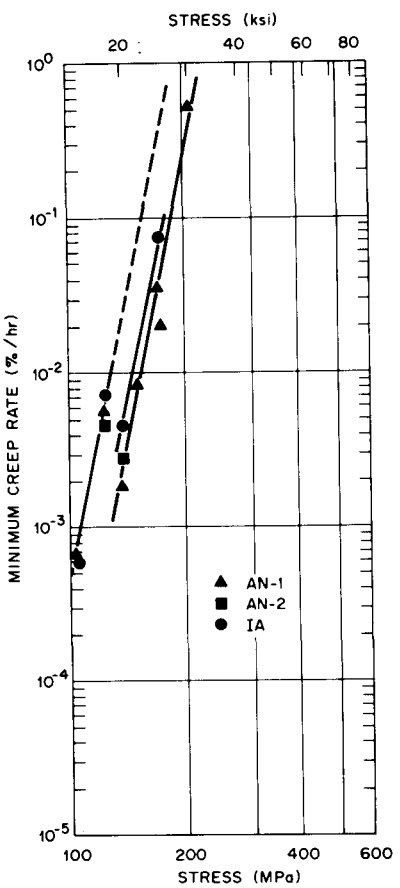

(*c*)

Fig. 3—Minimum creep rate as a function of stress for 2 1/4 Cr-1 Mo steel. (*a*) Tests on annealed and isothermally annealed plates at 454°C, (*b*) Tests on two fully annealed and one isothermally annealed steel at 510°C, (*c*) Tests on two fully annealed and one isothermally annealed steel at 566°C.

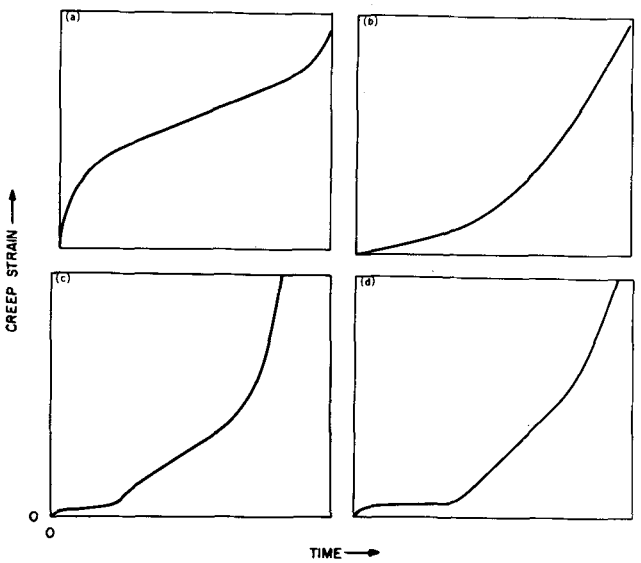

Fig. 4—Schematic diagrams of types of creep curves observed for annealed 2 1/4 Cr-1 Mo steel. (*a*) Classical creep curve, (*b*) Type of creep curve often observed, (*c*) and (*d*) Types of curves observed when the early portion of the curve in (*b*) is magnified.

(transient), secondary (steady-state), and tertiary creep stages. Many of the creep curves were as shown in Fig. 4(*b*). The test seemed to be immediately in tertiary creep, or at best, steady-state creep began at zero time, eventually going into an increasing creep rate (tertiary creep). However, when the first part of this curve was magnified, creep curves of the types shown schematically in Fig. 4(*c*) and (*d*) were observed. After a period of decreasing creep rate (transient creep), an apparent steady-state stage is reached, after which the creep rate begins to increase (tertiary creep?). Instead of increasing to rupture, however, the creep rate again decreases (Fig. 4(*c*)) and goes into what appears to be another steady-state stage (*i.e.*, creep rate is essentially constant). In

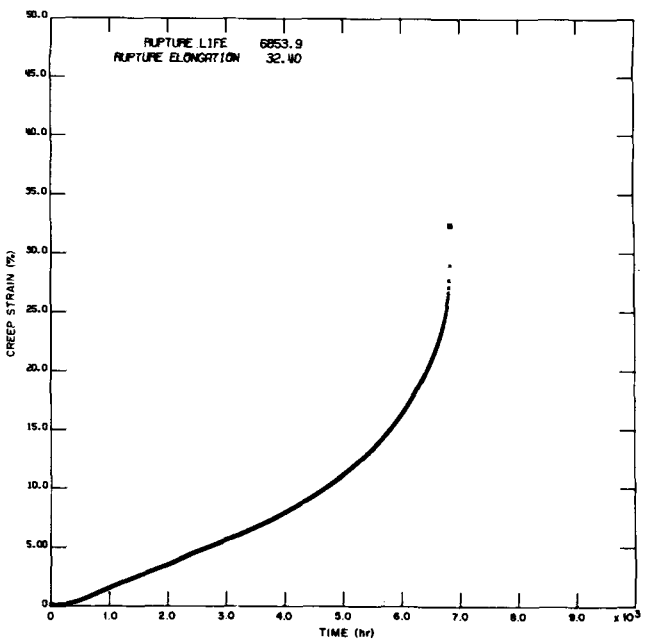

(*a*)

Fig. 5—Example of nonclassical creep curve for isothermally annealed 2 1/4 Cr-1 Mo steel tested at 152 MPa at 510°C. (*a*) Creep curve to rupture, (*b*) Creep curve to 5 pct.

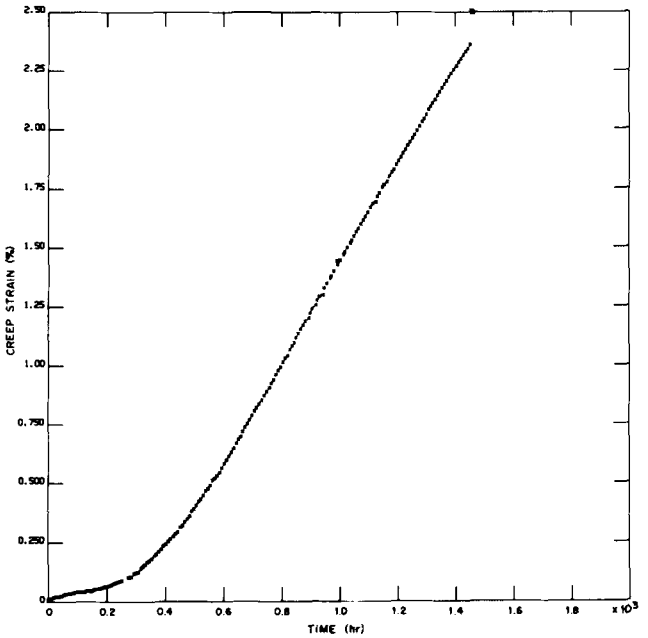

(*b*)

some instances the creep rate increases from the first steady-state stage directly into the second steady-state stage (Fig. 4(*d*)) (*i.e.*, no intermediate decreasing creep rate appears). Finally, after this second steady-state region, the creep rate again increases and continues to increase until rupture. Curves that have the two steady-state stages (Fig. 4(*c*) and (*d*)) will hereafter be referred to as nonclassical. For curves that showed nonclassical behavior, the creep rate for the first steady-state stage was plotted in Fig. 3.

An example of a nonclassical curve is that for an isothermally annealed specimen tested at 152 MPa (22 ksi) at 510°C (Fig. 5). When the entire curve is examined (Fig. 5(*a*)), it is found similar to Fig. 4(*b*). However, when only the first 5 pct is examined (Fig. 5(*b*)), we observe a nonclassical appearance similar to Fig. 4(*d*). The various creep stages are often more easily seen when the creep rate is plotted as a function of time on a double-logarithmic plot (Fig. 6). The two regions where the creep rate decreases and becomes constant are now quite obvious.

All creep curves were reexamined for shape and our observations are summarized schematically in Fig. 7. At 566°C, tests at 103 and 124 MPa for both heat treatments AN-1 and IA displayed classical creep curves. At 138 MPa a nonclassical creep curve was observed. The creep rate for the second steady-state creep stage was quite easily determined for the tests up to and including 172 MPa. At 207 MPa, however, we could only determine one creep rate, indicating a classical creep curve.

If the creep rate for the second steady-state region is plotted for the nonclassical creep curves at 566°C (stress ≥ 138 MPa), the points appear to fall on the extension of the curve for the tests at 103 and 124 MPa—the tests that displayed classical creep curves. This is shown in Fig. 8(*a*). Table V gives the data used for Fig. 8. Note that the 207 MPa test (the one where no second steady-state stage could be delineated) does not appear to fall on an extension of either of the two curves for AN-1.

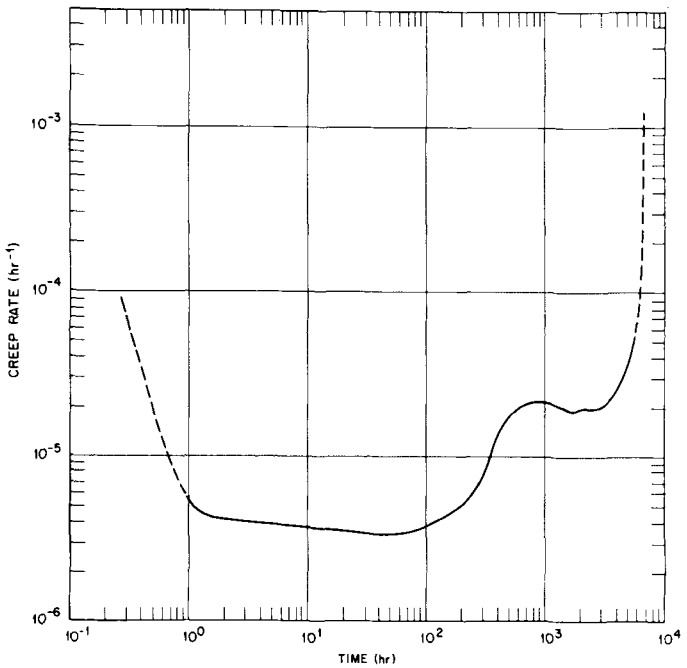

Fig. 6—Nonclassical creep curve from Fig. 5 replotted with creep rate given as a function of time.

Classical creep curves were observed for all the tests at 454°C (Fig. 7). At 510°C, the type of behavior depended on stress and heat treatment. For the AN-2 specimens at 510°C, all the creep curves appeared classical, except the one at 207 MPa. Although the creep curve at 207 MPa appeared nonclassical, it was very difficult to determine accurately the second steady-state stage creep rate because of the limited duration of this stage. However, a creep test (not ruptured) was made at 152 MPa that definitely had a nonclassical curve. Thus, we concluded that the boundary between classical and nonclassical curves for AN-2 was near 207 MPa.

All curves for AN-1 were nonclassical below about 241 MPa. Above this stress only a single steady-state stage could be accurately determined. For IA at 510°C, only nonclassical curves were observed, although the stresses tested were not as high as the highest stresses used for AN-1 and AN-2.

Figure 8(*b*) shows the data for the second steady-state stage creep rate at 510°C; the data used for this plot are given in Table V.

Figure 9 shows the elongation and reduction of area plotted against the rupture life at 454, 510, and 566°C.

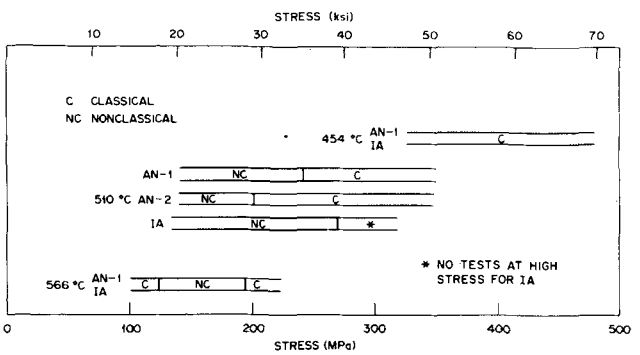

Fig. 7—Schematic representation of creep curve shape as a function of stress at 454, 510, and 566°C.

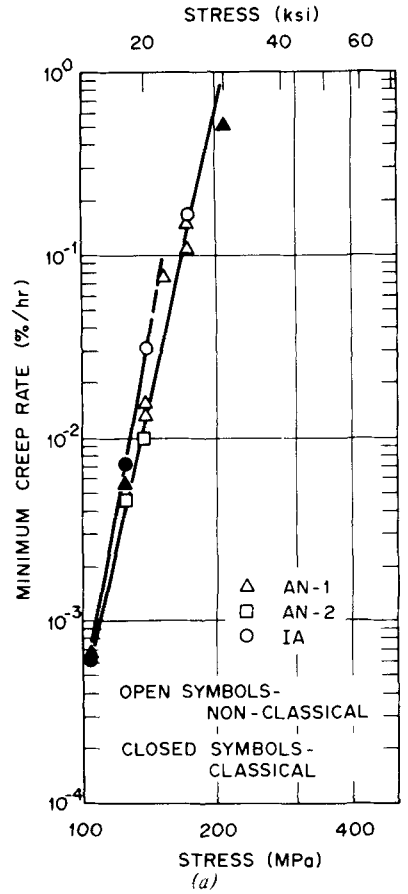

(*a*)

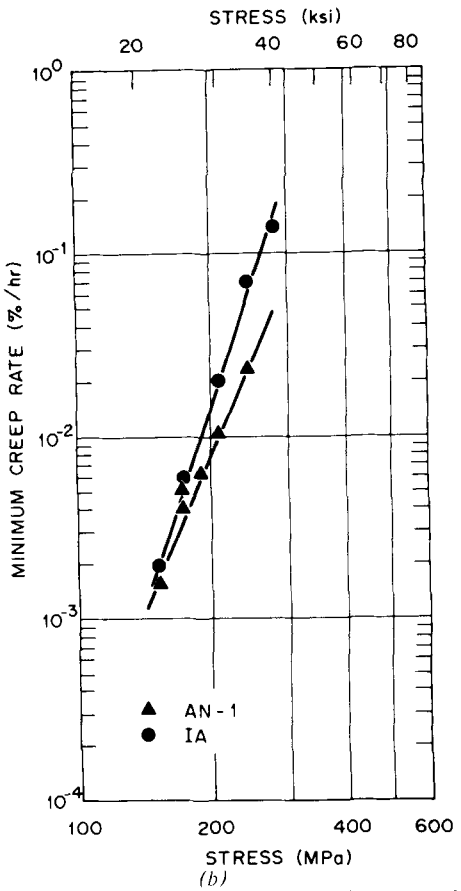

(*b*)

Fig. 8—Creep rate as a function of stress when second steady-state stage is plotted for nonclassical curves. (*a*) Heat treatments AN-1, AN-2, and IA at 566°C, (*b*) Heat treatments AN-1 and IA at 510°C.

Table V. "Steady-State Creep Rates" for Tests at 510 and 566°C

Stress, MPa	Creep Rate, Pct/h			
	AN-1		IA	
	Stage 1	Stage 2	Stage 1	Stage 2
		510°C		
152	0.000125	0.00153	0.000165	0.00196
172	0.0005	0.0042	0.000462	0.006
172	0.00053	0.00515		
189	0.00125	0.0061		
207*	0.0025	0.010	0.00339	0.021
241	0.0043	0.0235	0.00967	0.0702
276	0.0285	†	0.0397	0.141
310	0.071	†		
		566°C		
103	0.00065	†	0.000605	†
124	0.0055	†	0.00723	†
138‡	0.00187	0.0159	0.0175	0.0322
138	0.0033	0.013		
152	0.0086	0.076		
172	0.0375	0.150	0.075	0.17
172	0.0196	0.110		
207	0.51	†		

*The creep curves for the two 207 MPa tests for AN-2 were estimated to be nonclassical with creep rates of 0.000168, 0.0137 and 0.000167, 0.0030 pct/h.

†Classical creep curve; no second steady-state creep stage was distinguished.

‡Heat treatment AN-2 also displayed a nonclassical creep curve at 138 MPa and 566°C with creep rates of 0.00267 and 0.0099 pct/h.

Curves, which are meant only to show data trends, have been drawn. The ductility at 454°C (Fig. 9(*a*)) showed little change with rupture life. At 510°C (Fig. 9(*b*)), both the elongation and reduction of area appear

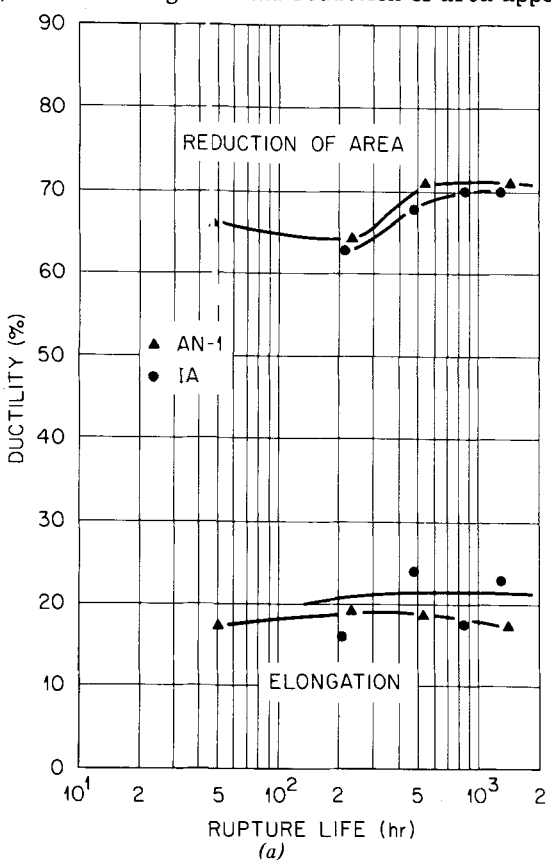

(*a*)

Fig. 9—Variation in rupture elongation and reduction of area with rupture time for annealed 2 1/4 Cr-1 Mo steel at (*a*) 454°C, (*b*) 510°C, and (*c*) 566°C.

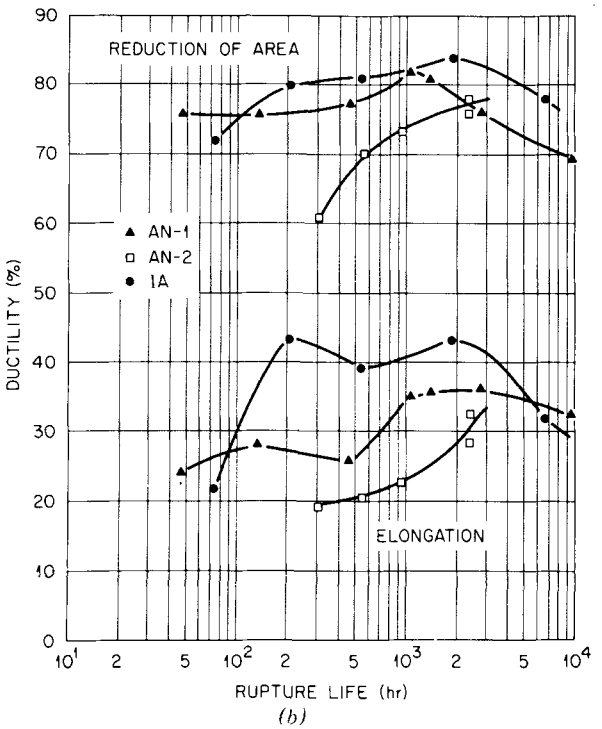

(*b*)

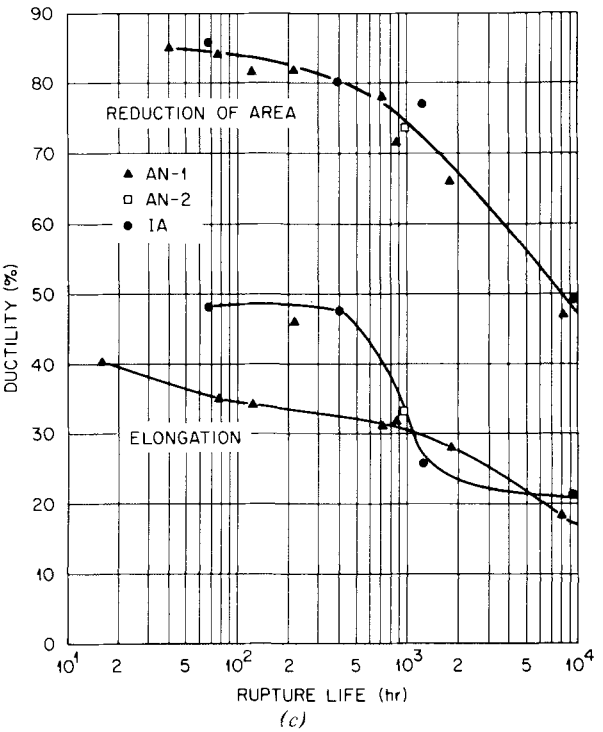

(*c*)

to go through a maximum with increasing rupture life. Although heat treatment AN-2 shows the least ductility over the stress range tested, it will apparently reach its maximum ductility at a longer rupture life than the other two heat treatments. For the 566°C data (Fig. 9(*c*)), the ductility appears to decrease rather continuously with increasing rupture life, with no apparent effect of heat treatment. The 454°C tests exhibited the least ductility, though the ductility of the short-time tests at 510°C approached similar values.

All the fractures at 454 and 510°C appeared by visual examination to be of the cup-cone type. Likewise, cup-cone failures were seen for the tests above 124

MPa at 566°C. As expected from the observation in Fig. 9(*c*), the specimens tested at 103 and 124 MPa (15 and 18 ksi) showed decreasing amounts of neck formation as the stress decreased (increased rupture life).

Metallographic examination of the fractured specimens generally agreed with the visual observations. At 454 and 510°C, the fractures were essentially entirely transgranular. Only at 566°C was there any indication of grain boundary separation, and here, only on the specimen tested at the lowest stress (103 MPa). However, even in this case there was considerable grain deformation, and the fracture was primarily transgranular.

DISCUSSION

From an examination of the creep-rupture curves at 510°C (Fig. 2), the large scatter observed when data are collected from various sources is now easily understood. For example, Smith's data compilation[2] for annealed 2 1/4 Cr-1 Mo steel shows that the rupture life at 138 MPa varies from 180 to 900 h and at 103 MPa from 700 to 10,000 h. The present data show that the slight difference in cooling rate used in this study can alter properties considerably. When data are compiled from different sources,[2] not only do differences in heat treatment affect the properties, but heat-to-heat variations in composition can also play a role. In reality, these chemical differences also give rise to heat treatment effects: composition changes affect the hardenability of the steel, which in turn affects the type of microstructure achieved during an anneal.

The metallurgical processes that cause strengthening in 2 1/4 Cr-1 Mo steel have been discussed[3] and can be used to explain the creep-rupture behavior. When steels contain substitutional and interstitial elements in solution that have an affinity for each other, these elements can interact to form atom pairs or clusters. Baird and Jamieson[4,5] showed that these clusters could form dislocation atmospheres that hinder dislocation motion and therefore strengthen the steel. They termed this process "interaction solid solution hardening." In annealed 2 1/4 Cr-1 Mo steel, we showed that interaction solid solution hardening is due to molybdenum and carbon interactions.[1,3]

During the anneal heat treatment, the proeutectoid ferrite that forms is supersaturated with respect to molybdenum and carbon. It is this molybdenum and carbon that gives rise to interaction solid solution hardening. With time at temperature, molybdenum and carbon are removed from solution to form Mo_2C, thus making it unavailable for further strengthening by interaction solid solution hardening. Once supersaturation is relieved, creep is controlled by the movement of dislocations through the ferrite matrix that contains a high density of Mo_2C precipitate particles.[3]

The steel that is cooled fastest during the anneal heat treatment will contain the largest amount of molybdenum and carbon in solution and will show the greatest interaction solid solution hardening effect. For this reason, AN-2 has the longest rupture life at the highest stresses. For the low-stress tests, molybdenum and carbon are being removed by precipitation during test, and less strengthening results from interaction solid solution hardening. This leads to the approach of properties for the three heat treatments at long rupture times (Fig. 3). Since the precipitation process is diffusion controlled, the approach of properties occurs most rapidly the higher the temperature, as observed when the results at 510 and 566°C are compared.

Since AN-2 has the highest molybdenum and carbon supersaturation, a higher density of Mo_2C precipitate could form, which would result in greater dispersion strengthening for this heat treatment. Hence, the strength advantage could persist beyond the time when strengthening is caused by interaction solid solution hardening. In the limit, however, the Mo_2C particles coarsen (Ostwald ripening), leading to a similarity of microstructures and similar strengths. Eventually, the Mo_2C for all heat treatments is replaced by eta-carbide and the final microstructures become the same for each: ferrite that contains large globular particles of $M_{23}C_6$ and eta-carbide[6] (the $M_{23}C_6$ forms in the parts of the microstructure that were bainite and pearlite after the heat treatment). However, this transformation of Mo_2C to more-stable carbides occurs only for tests with rupture times longer than those of the present study.

We previously explained the nonclassical creep curves.[3] The first steady-state stage was explained in terms of interaction solid solution hardening, where dislocation motion in creep is hindered by the interaction with molybdenum and carbon atoms or atom clusters. With time, the amounts of molybdenum and carbon in solution decrease until the interaction no longer hinders dislocation motion. Then the creep rate increases and eventually establishes a new steady state. In this new steady state, the creep rate is controlled by atmosphere-free dislocations moving through the Mo_2C precipitate field of the proeutectoid ferrite. Creep becomes classical below the stress at which the molybdenum and carbon atom clusters can diffuse with the moving dislocations.

A discontinuity in stress-minimum creep rate curve at 566°C (Fig. 3) resulted when the creep rates for the first steady-state stage for the nonclassical curves were plotted with the creep rates for the low-stress classical curves. The discontinuity coincided with the change from classical to nonclassical curves. However, when the creep rates for the second steady-state stage were plotted, good agreement was obtained (Fig. 8). This is expected, since in the latter case we are comparing creep rates for similar rate controlling processes (*i.e.*, dislocation motion through Mo_2C precipitates in proeutectoid ferrite).

For the tests at 454°C and the high-stress tests on AN-1 and AN-2 at 510°C, we previously concluded that the classical curves (Fig. 7) are different than the low-stress classical curves noted at 566°C.[3] The creep rate depends on dislocation density, which in turn depends on stress: the higher the stress, the larger the dislocation density. It was concluded, therefore, that above some stress, dislocations are generated faster than they can be tied up by molybdenum-carbon atom clusters. Hence, for the high-stress classical curves, the creep rate is determined by some combination of the processes that operate in

the two stages for materials that display nonclassical creep.[3]

At the highest stresses the large number of dislocations introduced during loading and primary creep determine the properties, independent of interaction solid solution hardening (*i.e.*, the small number of dislocations affected by atmospheres make up only a small portion of the total dislocation population). As the stress is lowered, a larger number of dislocations are affected by interaction solid solution hardening, and this process has a larger effect on the properties. This explanation can be used to account for the divergence of the properties of AN-1 and IA at 454°C (Figs. 1 and 2). For the high-stress tests at 510 and 566°C, the interaction solid solution hardening effect for AN-1 was greater than that for IA. A similar difference should also occur at 454°C. As the stress is decreased at 454°C, therefore, interaction solid solution hardening has a larger effect in AN-1 than IA, thus making AN-1 stronger. With time, precipitation will occur, and the properties will eventually converge.

The effect of stress on creep rate is generally analyzed according to the power law equation:

$$\dot{\epsilon} = A\sigma^n \exp(-Q/RT), \quad [1]$$

where $\dot{\epsilon}$ is creep rate, σ is the stress, A and n are constants, Q is the activation energy for creep, R is the gas constant, and T is the absolute temperature. Examination of the curves in Figs. 3 and 8 indicates that for a given temperature, n is a constant for both steady-state stages. However, n varies with temperature and heat treatment, and n is different for the two steady-state stages.

It is interesting to note that n appears to go through a minimum as the temperature is decreased from 566 to 454°C. The n values determined[13] from these tests are given in Table VI. Generally n decreases with decreasing temperature.[7] The reason for the minimum is not understood, but must involve the interaction solid solution hardening. We must therefore agree with Baird *et al*,[8] who concluded that for their ternary alloy an examination of the stress dependence and activation energy for creep to determine mechanisms can "give valuable information on alloys which are stable during the creep test, but for the type of alloys examined in the present work, where metallurgical changes occur during creep, measurements of stress dependence and activation energy are unlikely to give meaningful results."

Table VI. Stress Exponents for 2¼ Cr-1 Mo Steel Given Different Anneals

Heat Treatment	Stress Exponent, n				
		510°C		566°C	
	454°C	Stage 1	Stage 2	Stage 1	Stage 2
AN-1	20.6	8.3	5.6	12.1	11.1
IA	10.3	8.9	7.4	12.1	14.3
AN-2		6.7			

SUMMARY AND CONCLUSIONS

The effect of heat treatment on the creep and rupture properties of 2 1/4 Cr-1 Mo steel was investigated. Properties were determined at 454, 510, and 566°C on specimens taken from pieces of 25 mm thick plate (from a single heat of steel) given the following heat treatments: annealed (full anneal), labeled AN-1, which was slowly cooled from the austenitizing temperature, annealed, labeled AN-2, which was cooled at a faster rate, and isothermally annealed, labeled IA.

Cooling rate during the anneal heat treatment had a pronounced effect on the creep and rupture properties at 454 and 510°C. For short rupture times at 510°C, the creep strength of AN-2 was greater than AN-1, which in turn, was greater than IA. At longer rupture times, the properties for all three heat treatments approached a common curve. At 454°C, where only AN-1 and IA were tested, the creep-rupture and minimum creep rate curves deviated at long test times, with AN-1 becoming considerably stronger than IA. At 566°C, the creep-rupture properties for all three materials approached a common curve much more quickly than at 510°C.

The effect of heat treatment was attributed to differences in the precipitation state of the steels because of the variations in the anneal treatment. During the anneal treatment, the proeutectoid ferrite that formed was supersaturated with molybdenum and carbon. Molybdenum and carbon in solution gave rise to interaction solid solution hardening, a strengthening effect where molybdenum-carbon atom clusters form dislocation atmospheres. The faster the cooling rate during the heat treatment, the greater was the supersaturation and the greater the interaction solid solution hardening effect. Interaction solid solution hardening also gave rise to nonclassical creep curves. An examination of these curves allowed for an interpretation of the heat treatment effects on creep and rupture properties.

ACKNOWLEDGMENTS

The author gratefully acknowledges J. L. Griffith for carrying out the experimental work, R. T. King, A. J. Moorhead, C. R. Brinkman, and W. R. Martin for reviewing the manuscript, S. Peterson for editing, and Kathryn S. Witherspoon for typing.

REFERENCES

1. R. L. Klueh: *J. Nucl. Mater.*, 1977, vol. 68, pp. 294-307.
2. G. V. Smith: ASTM Data Ser. Publ., DS 6S2, ASTM, Philadelphia, March 1971.
3. R. L. Klueh: *Mater. Sci. Eng.*, 1978, vol. 35, pp. 239-53.
4. J. D. Baird and A. Jamieson: *J. Iron Steel Inst.*, 1972, vol. 210, pp. 841-46.
5. J. D. Baird and A. Jamieson: *J. Iron Steel Inst.*, 1972, vol. 210, pp. 847-56.
6. R. G. Baker and J. Nutting: *J. Iron Steel Inst.*, 1959, vol. 192, pp. 257-68.
7. R. Lagneborg: *Inter. Met. Rev.*, 1972, vol. 17, pp. 130-46.
8. J. D. Baird, A. Jamieson, R. R. Preston, and R. C. Cochrane: *Creep Strength in Steel and High-Temperature Alloys*, pp. 207-16, The Metals Society, London, 1972.